



**HAL**  
open science

## Dopamine functionalization of BaTiO<sub>3</sub>

Anshida Mayeen, Kala M. S., M. Jayalakshmy, Sabu Thomas, Didier Rouxel,  
Jacob Philip, R. Bhowmik, Nandakumar Kalarikkal

► **To cite this version:**

Anshida Mayeen, Kala M. S., M. Jayalakshmy, Sabu Thomas, Didier Rouxel, et al.. Dopamine functionalization of BaTiO<sub>3</sub>: an effective strategy for the enhancement of electrical, magnetoelectric and thermal properties of BaTiO<sub>3</sub>-PVDF-TrFE nanocomposites. Dalton Transactions, 2018, 47 (6), pp.2039-2051. 10.1039/C7DT03389C . hal-02277131

**HAL Id: hal-02277131**

**<https://hal.science/hal-02277131>**

Submitted on 10 Mar 2022

**HAL** is a multi-disciplinary open access archive for the deposit and dissemination of scientific research documents, whether they are published or not. The documents may come from teaching and research institutions in France or abroad, or from public or private research centers.

L'archive ouverte pluridisciplinaire **HAL**, est destinée au dépôt et à la diffusion de documents scientifiques de niveau recherche, publiés ou non, émanant des établissements d'enseignement et de recherche français ou étrangers, des laboratoires publics ou privés.

# **Dopamine functionalization of BaTiO<sub>3</sub>: An effective strategy for the enhancement of electrical, magnetoelectric and thermal properties of BaTiO<sub>3</sub>-PVDF-TrFE nanocomposite**

**Anshida Mayeen<sup>1</sup>, Kala M. S.<sup>2</sup>, Jayalakshmy M. S.<sup>3</sup>, Sabu Thomas<sup>3</sup>, Didier Rouxel<sup>4</sup>, Jacob Philip<sup>5</sup>, R. N. Bhowmik<sup>6\*</sup>, Nandakumar Kalarikkal<sup>1,3\*</sup>**

<sup>1</sup>*School of Pure and Applied Physics, Mahatma Gandhi University, Kottayam, Kerala, India-686 560*

<sup>2</sup>*Department of Physics, St. Teresa's College, Ernakulum, Kerala, India-682 011*

<sup>3</sup>*International and Inter University Centre for Nanoscience and Nanotechnology, Mahatma Gandhi University, Kottayam, Kerala, India-686 560*

<sup>4</sup>*Institut Jean Lamour-UMR CNRS 7198, Faculté des Sciences et Techniques, Campus Victor Grignard-BP 70239, 54506, Vandoeuvre-les-Nancy Cedex, France.*

<sup>5</sup>*Amal Jyothi College of Engineering, Kottayam, Kerala, India-686518.*

<sup>6</sup>*Department of Physics, Pondicherry University, R. Venkataraman Nagar, Kalapet, Pondicherry, India- 605014*

**\*Corresponding authors: [nkkalarikkal@mgu.ac.in](mailto:nkkalarikkal@mgu.ac.in) (Nandakumar Kalarikkal), [rnbhowmik.phy@pondiuni.edu.in](mailto:rnbhowmik.phy@pondiuni.edu.in) (R. N. Bhowmik)**

## **Abstract**

Electro-active polymer-ceramic composite systems are emerging materials in the fields of nanoelectronics, microelectromechanical and macroelectronic device applications. Still more precise and concise researches have yet to come in the areas of energy storage, harvesting, energy conversion etc. In line with this we have synthesized and analyzed PVDF-TrFE based nanocomposites of both functionalized and non-functionalized BaTiO<sub>3</sub> (BTO). All the samples were prepared as free standing films by employing solvent cast method. A systematic study in the structural, morphological, thermal, dielectric, ferroelectric, piezoelectric and magnetoelectric (ME) properties have been carried out. It has been analyzed that the addition of BTO nanoparticles (with and without functionalization) into the polymer matrix substantially improved the properties of the nanocomposite. By performing the above mentioned characterizations it could be proved that dopamine functionalized BTO (DBTO) samples are better choices for the above mentioned applications including magnetoelectric applications, than non-functionalized ones.

**Key words:** BaTiO<sub>3</sub>, PVDF-TrFE, dopamine, dielectric, piezoelectric, magnetoelectrics.

## 1. Introduction

Multifunctional materials are capable of sensing various peripheral magnetic, electrical, heat and optical impulses. They possess lots of applications in the present electronic devices such as sensors, actuators, memory and storage devices, etc. Main concern regarding these materials is the possibility of the room temperature performance<sup>1</sup>. In this scenario ferroelectric polymer based composite systems are gaining more attention because of their multifunctional properties. They exhibit different properties such as better piezoelectric, ferroelectric, dielectric, pyroelectric properties in addition to the good mechanical strength, etc. The materials with good dielectric constant, low dielectric loss and high breakdown voltage have been preferred for energy storage applications.<sup>2, 3</sup> In general, polymers possess low dielectric properties and good flexibility compared to ceramics. However, polymers alone cannot be used for energy storage applications due to low dielectric constants. Whereas ceramic materials (in our case BaTiO<sub>3</sub>) possess high dielectric constant, low breakdown strength and weak processability.<sup>4-6</sup> A very good solution is the incorporation of ceramic particles in polymer matrix and develop polymer-ceramic composites having high dielectric constant, low dielectric loss, as well as better breakdown strength.<sup>4,7-11</sup>

PVDF is a well-known electroactive polymer mainly due to its excellent ferroelectric property. PVDF and its co-polymers such as PVDF-TrFE, PVDF-HFP, etc. have been studied for a wide range of applications because of their, piezoelectric, pyroelectric and ferroelectric properties.<sup>12-17</sup> These polymers are widely used for non-volatile memory applications in electronic devices. Ferroelectric to paraelectric transition temperature in PVDF depends on several factors such as VDF content, heat treatment, poling, etc.<sup>17-18</sup> PVDF-TrFE possess additional advantages over the host polymer PVDF. It has much more crystallinity than that of parent polymer, PVDF and enhances the formation of  $\beta$ -phase without any additional processes such as stretching and poling.<sup>21,22</sup> In PVDF-TrFE the spontaneous polarization value is determined by the molar content of VDF and the crystallinity is determined by the content of TrFE. PVDF and its copolymers have shown ferroelectricity and good dielectric properties due to the presence of electronegative fluorine in the polymer chains and the spontaneous alignment of the polymeric chains.<sup>21-23</sup> From the application point of view, the main disadvantage is that, polymers possess low ferroelectric polarization and piezoelectric properties compared to ferroelectric ceramics. Lead based ceramics such as PbTiO<sub>3</sub> (PT), Pb(Zr,Ti)O<sub>3</sub> (PZT) and Pb(Mg<sub>1/3</sub>Nb<sub>2/3</sub>)O<sub>3</sub>-PbTiO<sub>3</sub> (PMN-PT) have been extensively studied for their large dielectric and piezoelectric constants.<sup>24</sup> In order to avoid the toxic lead based ceramics, the development of lead free ceramics were started to synthesize and are receiving

remarkable attention, out of which BaTiO<sub>3</sub> (BTO) is a preferable candidate due to its biocompatibility.<sup>25,26</sup> BaTiO<sub>3</sub> is the first developed piezoelectric ceramic, which shows a lot of interesting electrical properties including ferroelectric, piezoelectric, pyroelectric, magnetoelectric (ME) and optical properties.<sup>27,28</sup>

In the field of polymer-ceramic composite systems, active researches are going on to achieve high ferroelectric properties coupled with better dielectric properties and high degree of flexibility. So, presently, scientists and engineers are trying to fabricate actuators and sensors out of these composite materials.<sup>29-31</sup> Capacitors based on composites of BTO can play vital role in mobile electronics, where the materials can store huge amount of energy and discharge properly. Out of the polymer based composite ferroelectric systems, BTO-PVDF-TrFE can play a significant role in future technology due to its enhanced electromechanical coupling, piezoelectric, ferroelectric, mechanical and dielectric properties along with its biocompatibility.<sup>32</sup> Moreover the multiferroic/ magnetostrictive ceramic fillers like BaTiO<sub>3</sub>, CoFe<sub>2</sub>O<sub>4</sub>, BiFeO<sub>3</sub>, ZnFe<sub>2</sub>O<sub>4</sub> etc., incorporated in ferroelectric polymer matrix offer a new prospect for the development/ fabrication of ultramodern devices in the field of magnetoelectrics.<sup>33-39</sup> Presently, the area of research dealing with ME coupling and associated properties which still have a lot of mysteries, possibilities, and challenges is an interesting area of research for scientists and engineers world-wide.<sup>33-35</sup>

Instead of single phase multiferroics/magnetoelectrics, composite magnetoelectric systems are generally preferred to the technological applications. Due to the lack of mechanical stability, ceramic magnetoelectric composite systems cannot be considered for high end magnetoelectric applications. In this regard, electroactive polymer based magnetoelectrics can contribute more to the field of magnetoelectrics. In polymer based magnetoelectric materials, magnetic field induces a dimensional change in the magnetostrictive material that is transferred to the adjacent piezoelectric material, which subsequently creates a mechanically induced polarization.<sup>36</sup> Since BaTiO<sub>3</sub> is a multiferroic material which possesses induced magnetism<sup>28</sup>, incorporating these kinds of ceramic materials in electroactive polymer matrices offers comparatively high magnetoelectric response with high degree of flexibility, which is highly preferred to the technological applications. Here such kind of polymer based magnetoelectric material using BTO nanoparticles incorporated in PVDF-TrFE co-polymer matrix with varying filler concentrations has been prepared, which could be a suitable candidate for the development of smart magnetoelectric devices. This composite system which possesses various properties,

offer a new perspective for the development of energy storage, harvesting and smart magnetoelectric device applications.<sup>17,21,32,33-38</sup>

From the point of view of material synthesis, the addition of ceramic nanofillers into polymer matrices (organic–inorganic hybrids) causes an aggregation of nanoparticles because of the large surface energy of the filler particles and it subsequently produces inhomogeneity in the nanocomposite. This agglomeration and inhomogeneity increases with filler concentration in the polymer matrix and leads to a lack of perfection in controlling the electrical properties of the entire composite system. This problem can be resolved up to a certain limit by the functionalization of nanoparticles.<sup>31,39</sup> Such technique will help to increase the compatibility between the nanoparticles and polymer matrix. From literature<sup>40</sup> it could be notice that, researchers tried with different coupling groups such as silane groups, phosphonates and catechols (e.g. dopamine) to improve the nanoparticles-polymer compatibility.

In the present work, a comparative study of the electrical properties of BaTiO<sub>3</sub>-PVDF-TrFE (BTO-PVDF-TrFE) nanocomposites before and after functionalization of BTO particles using Dopamine has been performed. BTO nanoparticles were prepared by Pechini method and functionalized using Dopamine Hydrochloride. Compared to linear linking agents, dopamine is a better choice for the functionalization of BaTiO<sub>3</sub>. It will act as a bridge between the filler and the polymer matrix. OH group of dopamine will attach to the surface of BaTiO<sub>3</sub> and at the same time NH group will bind on C-F group of the PVDF-TrFE polymer.<sup>32,40-41</sup> Hence, compatibility between the nanoparticles and the polymer will be enhanced. Moreover, multiple OH groups on the surface of BaTiO<sub>3</sub> will undergo some reaction with phenol groups present in the side chain of dopamine, resulting in the formation of multiple benzene groups near to the surface of the nanoparticles. Thus, this functionalization can prevent aggregation to a greater extent. This reduction in aggregation will play a key role in improving the electrical properties.<sup>30,41</sup> The nanocomposite films were prepared by solvent cast method with varying concentration of BTO in the polymer matrix. The dielectric, piezoelectric, magnetoelectric and thermal properties of the prepared films for both functionalized and non-functionalized samples have been characterized and the results are compared.

## 2. Experimental

### 2.1. Preparation of BTO nanoparticles

The BTO nanoparticles were prepared by Pechini method using barium acetate ACS reagent (99%), titanium (IV) isopropoxide (97%), citric acid anhydrous and ethylene glycol as raw materials. Stoichiometric quantities of barium acetate ( $\text{Ba}(\text{C}_2\text{H}_3\text{O}_2)_2$ ) and titanium isopropoxide ( $\text{Ti}[\text{OCH}(\text{CH}_3)_2]_4$ ) were added to citric acid solutions in separate beakers. Both solutions were stirred at  $60^\circ\text{C}$  for 1h. When they became transparent, ethylene glycol was added and mixed well. Then, the solutions were mixed together and the obtained solution was heated at  $90^\circ\text{C}$  until it forms a gel with pale yellow colour. After that, the heating temperature was increased to  $120^\circ\text{C}$  to form a brown glassy resin. It was then kept in an oven and heated at  $300^\circ\text{C}$ ,  $500^\circ\text{C}$ , and  $700^\circ\text{C}$  each for 4h followed by high temperature sintering ( $1200^\circ\text{C}$ ) to obtain BTO nanoparticles with tetragonal crystal structure.

### 2.1. Dopamine Functionalization of BTO nanoparticles

The prepared BTO nanoparticles were functionalized using dopamine hydrochloride. 10 mm concentration dopamine hydrochloride is used for the functionalization of  $\text{BaTiO}_3$ .

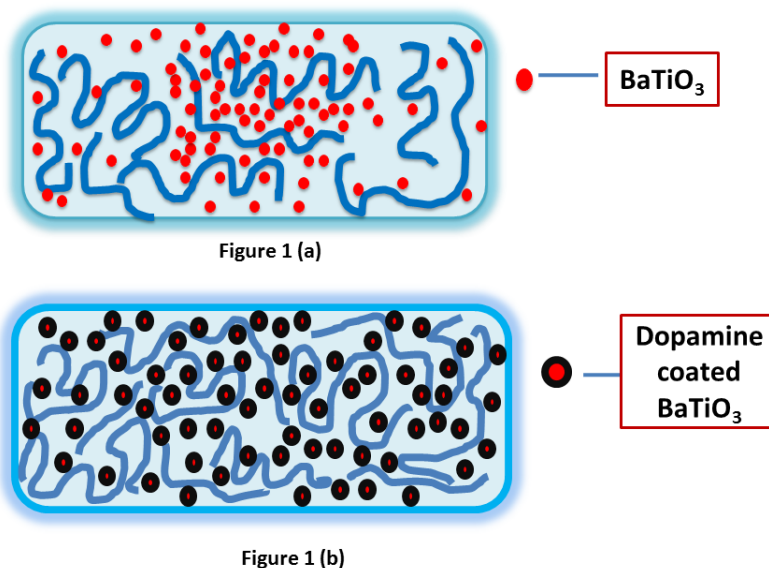


**Figure 1:** Schematic diagrams of the interaction of BTO nanoparticles with PVDF-TrFE matrix prior to functionalization (a) and dopamine functionalized BTO nanoparticles with PVDF-TrFE(b).

Dopamine hydrochloride and BTO nanoparticles were added to distilled water and magnetically stirred at room temperature and dried at  $60^\circ\text{C}$  in vacuum to avoid oxidation of dopamine for 10 h followed by an ultra-sonication for 30 min. After that the resultant solution

was centrifuged, dried and ground well. Finally, we got a black coloured coating over the BTO nanoparticles which was white in colour.

Schematic diagrams of the interactions of both functionalized and non-functionalized BTO nanoparticles with PVDF-TrFE are shown in Fig. 1. Dopamine functionalized BTO in PVDF-TrFE shows good dispersion and the distribution of nanoparticles is uniform without agglomeration. Unfunctionalized BTO in PVDF-TrFE matrix will have the tendency to form agglomerates and the distribution of the particles in the polymer matrix will be comparatively poor.

### **2.3. Composite film preparation**

The BTO/DBTO-PVDF-TrFE composite film samples with varying filler concentrations (2%, 4%, 8%) were prepared by solvent cast method. For all the composite film samples, 15 wt% PVDF-TrFE (70/30 from Piezotech, France) polymer solution was used. The methyl ethyl ketone (MEK) was used as solvent. The polymer-ceramic mixture was continuously stirred for 2 h at 50 °C followed by sonication for 30 min. The mixture was then transferred to a petridish and kept for 4 days at room temperature for the complete evaporation of the solvent. Finally, the films were peeled off from the petridish. Such prepared film samples were heated at 138 °C to ensure the  $\beta$ -crystalline phase of PVDF-TrFE. Thickness of the films prepared were found to be in the range of 180 - 200  $\mu\text{m}$ . Schematic diagram illustrating the preparation of the DBTO-PVDF-TrFE films is shown in Fig 2. The composite film samples with dopamine functionalized BTO are expected to have good compatibility with the PVDF-TrFE due to binding of the OH group of the filler with the OH group of dopamine. Similarly, NH group of dopamine will bind to the C-F group of PVDF-TrFE. <sup>31,32,39-41</sup>

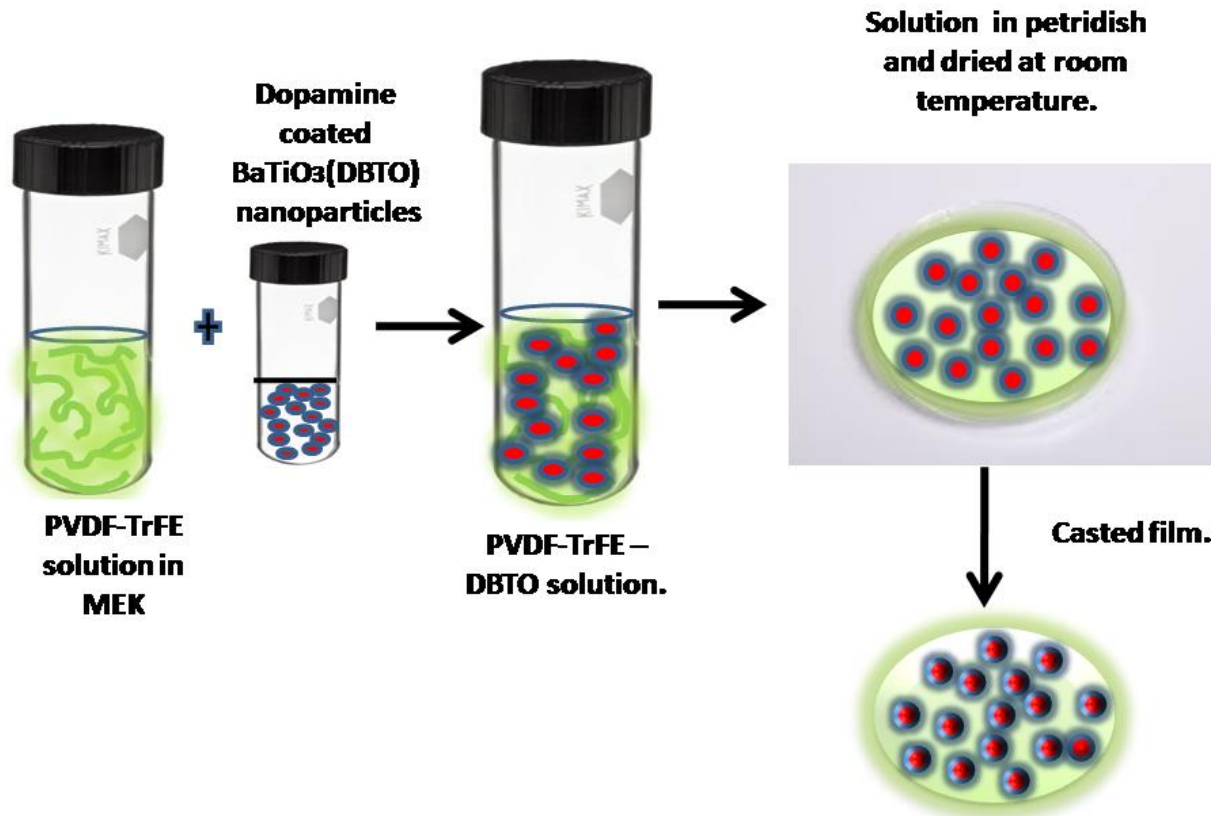


*Figure 2: - Schematic diagram showing the preparation of DBTO-PVDF-TrFE films*

#### 2.4. Material characterization

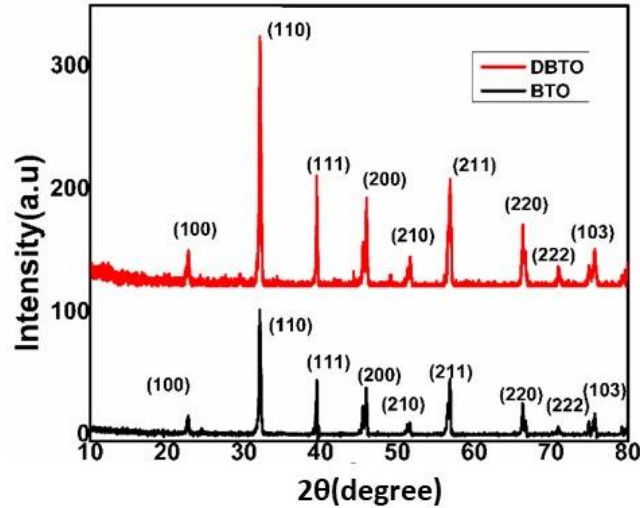
Crystal structure analysis of the samples was carried out by using Philips X'Pert PRO XRD with Cu-  $K\alpha$  line (wavelength 1.54 Å). XRD data were obtained for  $2\theta$  values ranging from 10 to 80°. Powders of BTO, DBTO and prepared film samples were also analyzed using Fourier transform infrared microscopy (FTIR) using Perkin Elmer's Spectrum 400 FTIR spectrometer. Micro-Raman spectra were recorded using Witech Alpha 300 R-A Confocal spectrometer. Transmission electron microscopic (TEM) images of the DBTO particles were taken by transmission electron microscope, JEOL's JEM 2100. Field emission scanning electron microscopic (FE-SEM) images of the samples were taken by using Nova Nano SEM 450. Dielectric properties (Dielectric constant, loss, ac conductivity) were measured by using LCR meter (Agilent E4980A). The piezoelectric measurement of the composite films was carried out by using Berlincourt Piezometer PM300 and  $d_{33}$  coefficients were recorded. The films were poled before piezoelectric measurement by means of corona poling unit, where poling was carried out at 14.5 kV/cm electric field for 30 min. Ferroelectric properties were measured by using a P-E loop tracer (Radiant technologies). For the ME measurements, a lock in amplifier method has been employed. Thermal properties such as thermal

conductivity and specific heat capacity were studied by employing a photopyroelectric (PPE) technique using a home built set up, in which a lock in amplifier, mechanical chopper and a He-Cd laser are used. The laser source is used to heat the sample optically. A mechanically chopped beam of radiation from the laser source falls on the sample. A part of the incident radiation is absorbed by the sample and undergoes a radiative de-excitation process and it results in heating the sample. The variation of temperature experienced by the sample can be detected with the help of a pyroelectric transducer kept in intimate contact with the sample.<sup>42,43</sup> PVDF film coated with Ni-Cr alloy having a pyroelectric coefficient  $30\mu\text{C}/\text{m}^2\text{K}$  was used as the pyroelectric detector. The sample-detector assembly was placed on a thermally thick copper backing. The modulation frequency was set above 60 Hz to ensure the sample-detector-backing assembly in a thermally thick regime. The output signal was measured using a dual phase lock in amplifier in the form of amplitude and phase. From the amplitude and phase measurements thermal effusivity and thermal diffusivity of the samples were evaluated; as a result, thermal conductivity and specific heat capacity values could be calculated.<sup>42,43</sup>

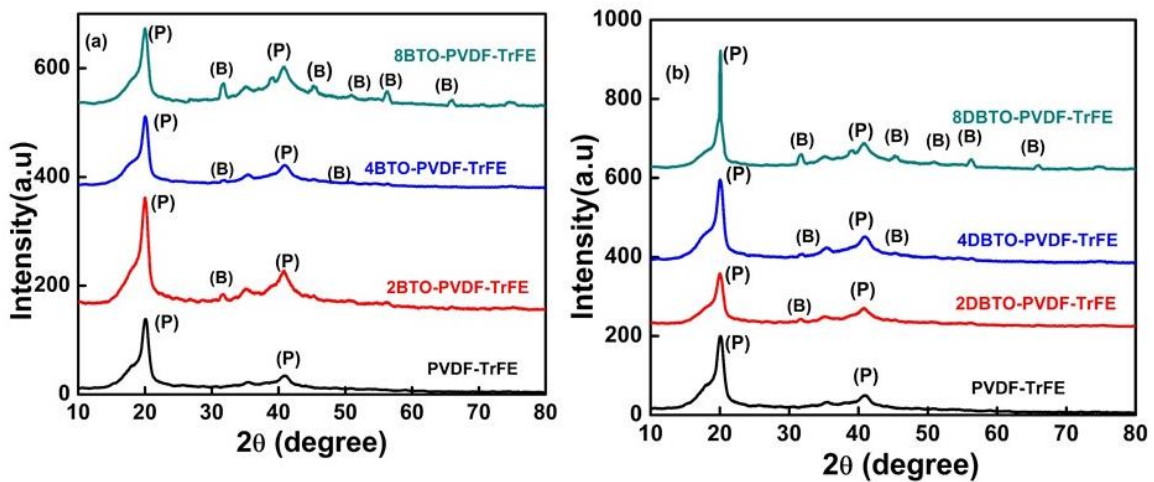
### **3. Results and Discussions**

#### **3.1. Micro-structural properties**

The crystalline structure of the prepared  $\text{BaTiO}_3$  sample was determined by using XRD pattern (Fig. 3). The tetragonal phase of  $\text{BaTiO}_3$  was confirmed by comparing the observed pattern with the JCPDS (# 073644) ICDD pattern. The splitting up of the peak at  $45^\circ$  in both the XRD pattern of BTO and DBTO is caused due to off - centering of  $\text{Ti}^{4+}$  ions, attributing to tetragonal non- centrosymmetric phase in  $\text{BaTiO}_3$ . The peak intensity in DBTO particles is found more than the non-functionalized (as-prepared) BTO particles. The average size of  $\text{BaTiO}_3$  particles was calculated from Scherrer equation  $D = k\lambda/\beta\text{Cos}\theta$  and was found to be nearly 141nm and 158nm for non-functionalized BTO and DBTO samples, respectively.

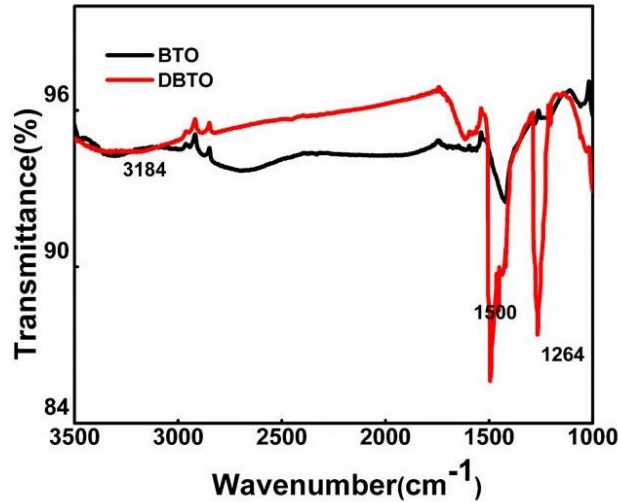


**Figure 3.** XRD patterns of  $BaTiO_3$  (BTO) nanoparticles and dopamine functionalized  $BaTiO_3$  (DBTO) nanoparticles.



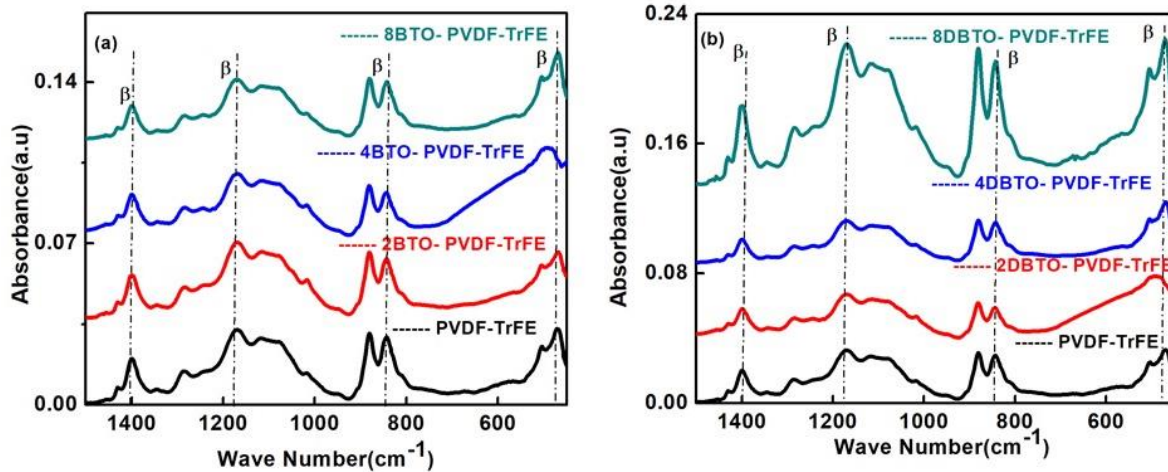
**Figure 4.** XRD patterns of BTO-PVDF-TrFE (a) and DBTO-PVDF-TrFE (b) casted films.

Fig. 4 shows the XRD pattern of the composite film (non-functionalized and functionalized) samples. The peaks of the polymer PVDF-TrFE are represented by ‘P’ and that of the  $BaTiO_3$  is represented by ‘B’. The peak at  $20.50^\circ$  in the XRD pattern of the film samples represents the reflection from (110) and (200) planes of the beta polar phase of PVDF-TrFE. Peaks of BTO are more visible in the XRD pattern of composite films, containing more than 2 wt% of BTO and DBTO nanoparticles. XRD pattern of the films with filler concentration 4% and 8% (4BTO, 4DBTO, 8BTO, 8DBTO) shows an additional peak at  $45^\circ$ , which confirms the presence of tetragonal phase of  $BaTiO_3$  in the composite films. Fig.5 shows the FTIR spectra of Barium Titanate nanoparticles before and after functionalization. Additional bands of DBTO at  $3184\text{ cm}^{-1}$  are attributed to N-H stretching



**Figure 5.** FTIR spectra of functionalized and unfunctionalized Barium Titanate nanoparticles.

vibration,  $1500\text{ cm}^{-1}$  are assigned to the benzene ring C-C vibration, and band at  $1264\text{ cm}^{-1}$  corresponds to the C-O stretching of phenolic O-H group, which shows that dopamine was successfully coated over the surface of barium titanate nanoparticles.<sup>44-46</sup>



**Figure 6.** FTIR spectra of BTO-PVDF-TrFE (a) and DBTO-PVDF-TrFE (b) casted films.

Fig. 6 depicts the FTIR spectra of the film samples. Vibration bands of the composite films were studied in the wave number range  $700\text{--}1500\text{ cm}^{-1}$  range. The prominent peaks at  $1285\text{ cm}^{-1}$ ,  $860\text{ cm}^{-1}$ , and  $1400\text{ cm}^{-1}$  confirm the beta phase of polymer in the composite samples. The peak observed at  $1285\text{ cm}^{-1}$  corresponds to  $\text{CF}_2$  asymmetric stretching, C-C symmetric stretching and CCC scissoring vibration in the  $\beta$ - phase of PVDF-TrFE. C-F asymmetric stretch is highly dependable on the ferroelectric crystallinity. Band at  $860\text{ cm}^{-1}$  corresponds to the symmetric stretching of the  $-\text{C-F}$  and plane rocking of  $-\text{CH}_2$  respectively, both bands the

wagging frequency of  $-\text{CH}_2$  bond and C-C asymmetric stretch. From the FTIR spectra, it is clear that all additional phases other than beta is absent in the composite films.

47-49

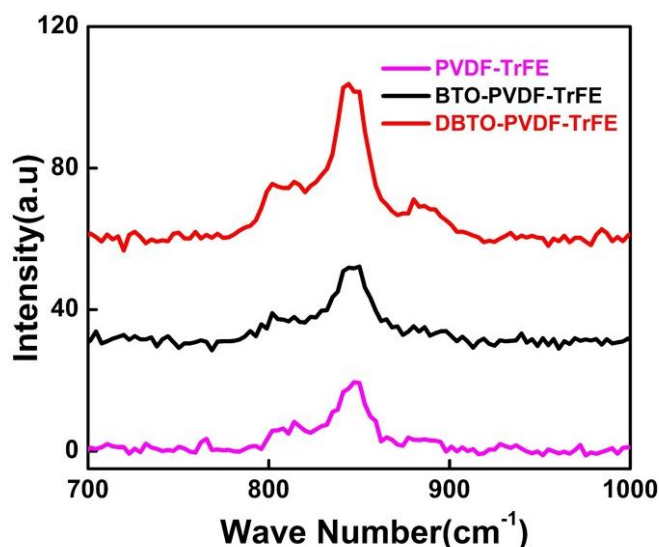


**Figure 7. Confocal Raman spectra of pure PVDF-TrFE, BTO-PVDF-TrFE and DBTO-PVDF-TrFE films.**

In the Confocal-Raman spectra shown in Fig. 7, the band at  $840\text{ cm}^{-1}$  also confirm the  $\beta$ -crystalline phase of the matrix. From XRD, FTIR and Raman data it can be seen that the addition of BTO/DBTO nanoparticles doesn't alter the ferroelectric  $\beta$ -phase of the PVDF-TrFE.<sup>34</sup>

The TEM images of dopamine coated  $\text{BaTiO}_3$  are shown in Fig. 8. From Fig. 8(a), it is clear that the DBTO particles are almost uniform size with an average particle size of  $\sim 158\text{ nm}$ , which is in good agreement with the XRD results. A uniform coating of dopamine over the BTO surface with a coating thickness of  $\sim 9\text{ nm}$  can be clearly observed in Fig. 8(b).<sup>39,41</sup> HR-TEM image shown in Fig 8(c) exhibits two different regions (separated by red dots). Lattice planes of  $\text{BaTiO}_3$  are shown by the region inside the red boundary and dopamine coated region is exposed outside, the d-spacing values of  $0.23\text{ nm}$  and  $0.41\text{ nm}$  corresponds to the (111) and (001) planes of  $\text{BaTiO}_3$  nanoparticles respectively [JCPDS PDF#812203]. Circular bright rings in the selected area electron diffraction (SAED) pattern in Fig 8(d) suggests that the particles are nanocrystalline.<sup>28</sup>

The FE-SEM images in Fig. 9(a) and 9(b) suggest almost uniform sized particles in the prepared  $\text{BaTiO}_3$  samples with average particle size  $\sim 136\text{ nm}$ . The images give evidences for the formation of cubic structured  $\text{BaTiO}_3$  nanoparticles. The FE-SEM image in Fig. 9(c)

confirms that cubic shape of the particles of non-functionalized BTO is changed to spherical shape after functionalization and the average size of the particles is increased to 161 nm. This change in the shape of the nanoparticles can be explained on the basis of the hydroxyl group formation on the surface of the nanoparticles with the dopamine. The particle size of the BaTiO<sub>3</sub> after functionalization is also increased due to the dopamine coating on the surface of the particles. Moreover, the particle sizes of BaTiO<sub>3</sub> and dopamine modified BaTiO<sub>3</sub> obtained from the FE-SEM image are in good agreement with the particle size calculated from XRD. By analyzing the FE-SEM images of the PVDF-TrFE film Fig. 9(d), BTO-PVDF-TrFE film Fig. 9(e) and DBTO-PVDF-TrFE film Fig. 9(f), one can see the distribution of nanoparticles in the polymer matrix. The BTO nanoparticles showed a tendency of aggregation in the polymer matrix, but in the case of dopamine functionalized samples, the particles showed uniform distribution without much aggregation

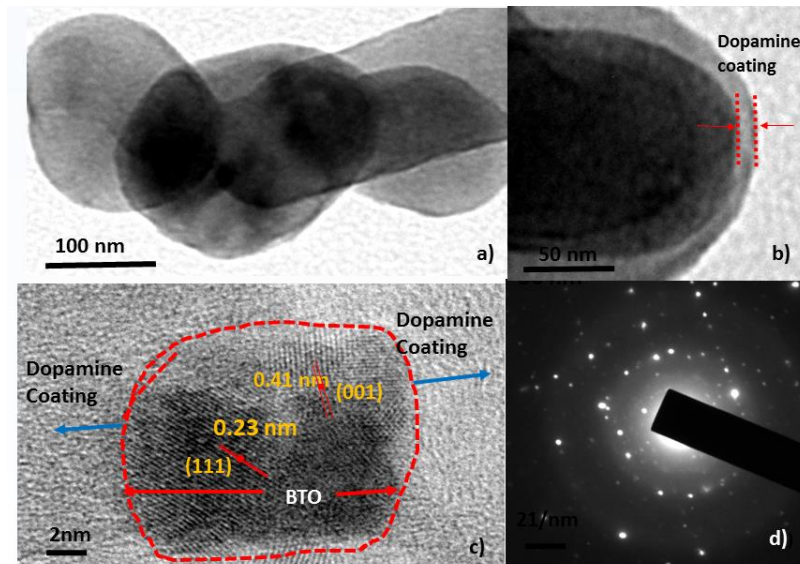


**Figure 8.** TEM images of Dopamine Functionalized Barium Titanate nanoparticles (a) and (b) TEM images, (c) HR-TEM image of DBTO, (d) SAED pattern of DBTO.

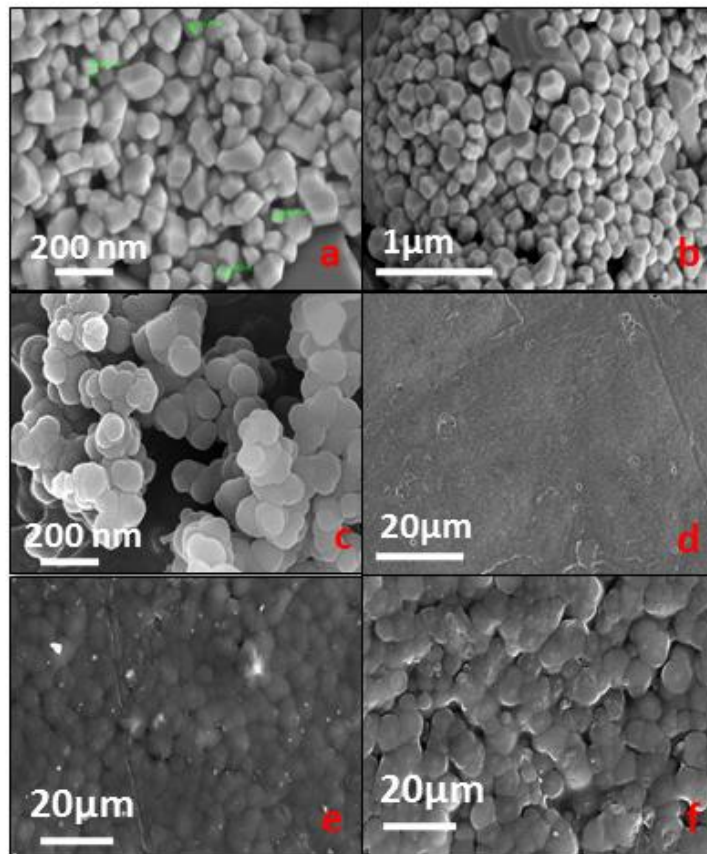


*Figure 9. FE-SEM images for the prepared BaTiO<sub>3</sub> nanoparticles (a&b), dopamine functionalized BaTiO<sub>3</sub> particles (c), neat PVDF-TrFE film (d), the distribution of unfunctionalized BaTiO<sub>3</sub> nanoparticles in the PVDF-TrFE matrix (e) and the distribution of dopamine functionalized BaTiO<sub>3</sub> particles in the polymer matrix (f).*

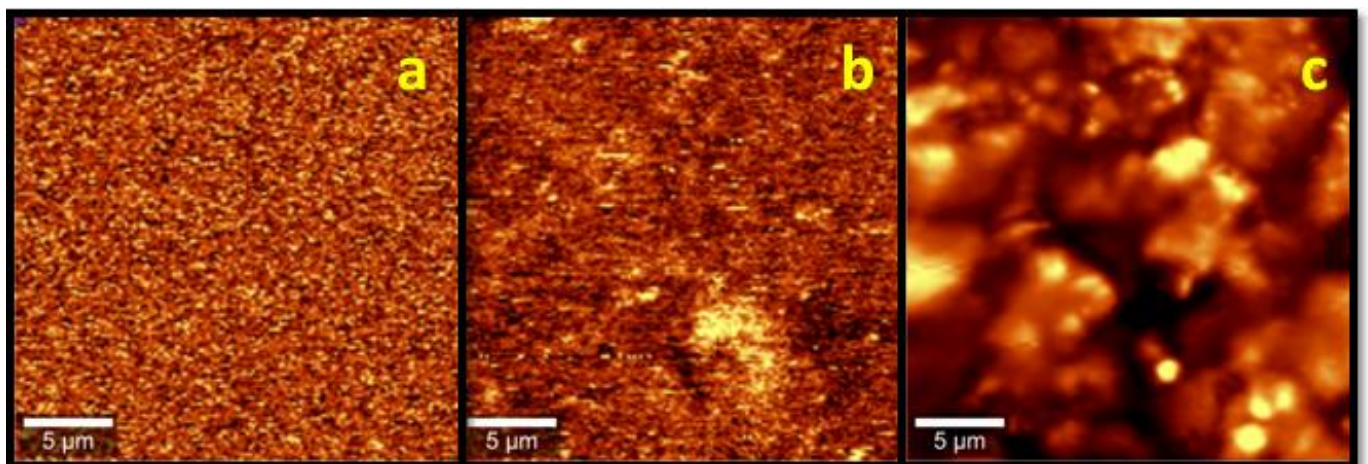


*Figure 10. Confocal Raman images for the PVDF-TrFE film (a), BTO- PVDF-TrFE film (b) and DBTO- PVDF-TrFE film.*

Fig.10 shows the Confocal Raman images of the prepared films. From the above Raman images, it is clear that DBTO-PVDF-TrFE composite film shows better surface compatibility

than the BTO- PVDF-TrFE nanocomposite film. Since dopamine act as a bridge between nanoparticles and the polymer matrix, the interaction between them has increased, and subsequently compatibility also increases.

The surface roughness of the Pure PVDF-TrFE, BTO-PVDF-TrFE and DBTO-PVDF-TrFE casted films is examined by atomic force microscopy (AFM) technique, and is depicted in Fig. 11(a-c) respectively. Addition of ceramic particles in the polymer matrix increase the

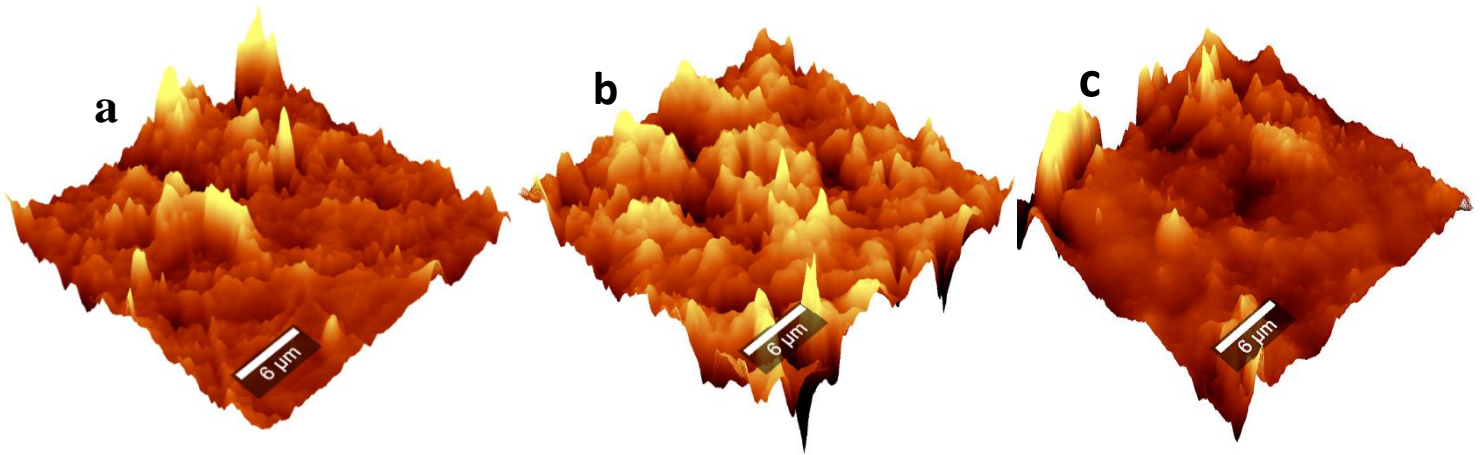


**Figure 11. AFM images of (a) Pure PVDF-TrFE (b) 8BTO-PVDF-TrFE and (c) 8DBTO-PVDF-TrFE casted films.**

surface roughness.<sup>50</sup> The surface roughness of the 8DBTO- PVDF-TrFE (17 nm) and 8BTO- PVDF-TrFE (26 nm) films are higher than that of the pure PVDF-TrFE films (8 nm). Although the roughness of the films has been increased by the addition of filler, but the DBTO-PVDF-TrFE films possess much lower surface roughness than BTO-PVDF-TrFE films. Thus, dopamine functionalization of BaTiO<sub>3</sub>, herein controls the surface roughness of the films, which is crucial for the electronic applications.<sup>51</sup>

### **3.2. Thermal conductivity and heat capacity**

Materials with good thermal conductivity are preferred to electronic applications mainly for controlling the heat energy loss.<sup>52</sup> The thermal conductivity of BTO-PVDF-TrFE and DBTO-PVDF-TrFE films with different filler (BTO) content has been measured. Fig. 12(a) shows that as the concentration of the BTO nanoparticles in the polymer matrix increases, the thermal conductivity of the composite film increases.

Thermal conductivity of the neat polymeric sample is found to be 0.34 W/mK and reaches a maximum value of 0.43 W/mK for 8% DBTO-PVDF-TrFE film. The thermal conductivity of the functionalized DBTO-PVDF-TrFE films is found higher than that in non-functionalized films. Increase in thermal conductivity of DBTO-PVDF-TrFE is attributed to the strong interfacial interaction between the polymer and the filler, which reduces interface thermal resistance of the composite films.<sup>53</sup>

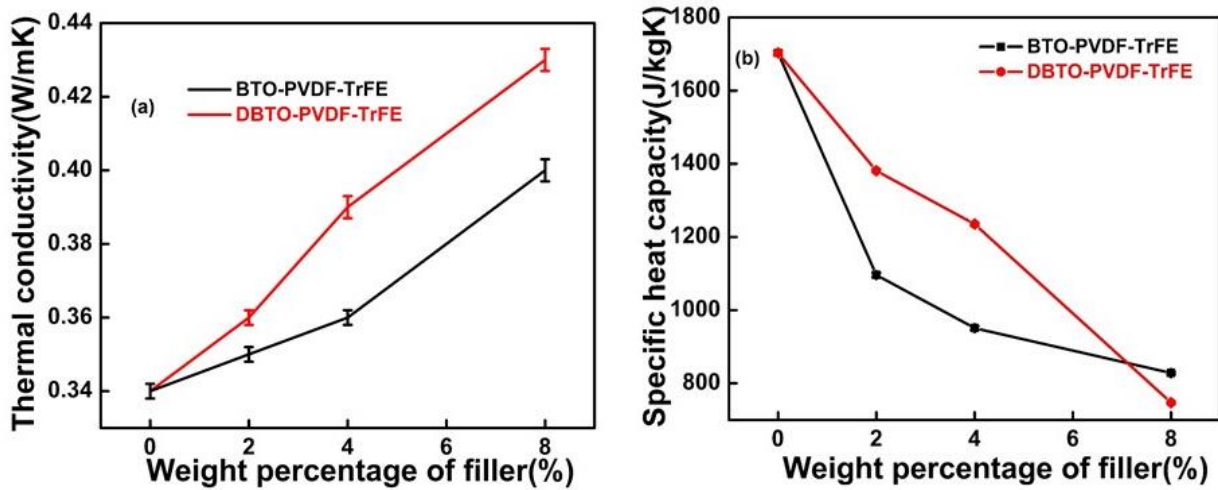


**Figure 12. (a) Variation of thermal conductivity and (b) variation of specific heat capacity of the films of BTO-PVDF-TrFE and DBTO-PVDF-TrFE with different filler content.**

The enhancement of crystallinity in the composite film in the presence of ceramic filler also effects on the enhancement of thermal conductivity in composite samples. On the other hand, Fig.12(b) shows that the specific heat capacity of the composite films decreases, with the increase in filler concentration (BTO and DBTO). This decrease in specific heat capacity of the composite films were due to relative arrangement of the fillers in the polymeric matrix.<sup>42</sup>. Variation of thermal conductivity and specific heat capacity of the composite films with different BTO/DBTO concentration are shown in table 1. The specific heat capacity of neat polymeric sample is found to be 1703 JKg<sup>-1</sup>K<sup>-1</sup>. The BTO-PVDF-TrFE nanocomposite film with 8wt % of filler concentration shows specific heat capacity around 828 JKg<sup>-1</sup>K<sup>-1</sup> whereas the 8wt% of filler in DBTO-PVDF-TrFE nanocomposite film shows specific heat capacity about 747 JKg<sup>-1</sup>K<sup>-1</sup>. Similar behavior in thermal conductivity and specific heat capacity have been reported by J. Philip et.al.<sup>42,43,54</sup>

**Table 1: - Calculated thermal conductivity and specific heat capacity of BTO-PVDF-TrFE and DBTO-PVDF-TrFE nanocomposite films.**

Sample Name	Thermal conductivity (W/mK)	Specific heat capacity (J/Kg K)
PVDF-TrFE	0.34	1703
2BTO-PVDF-TrFE	0.35	1096
2DBTO-PVDF-TrFE	0.36	1381
4BTO-PVDF-TrFE	0.36	951
4DBTO-PVDF-TrFE	0.39	1235
8BTO-PVDF-TrFE	0.40	828
8DBTO-PVDF-TrFE	0.43	747

### 3.3. Electrical properties

Electrical properties of the polymer nanocomposites depend upon the dispersion of the fillers in the polymeric matrix, composite making process, particle size of the fillers, and properties of the matrix, etc.<sup>55,56</sup>

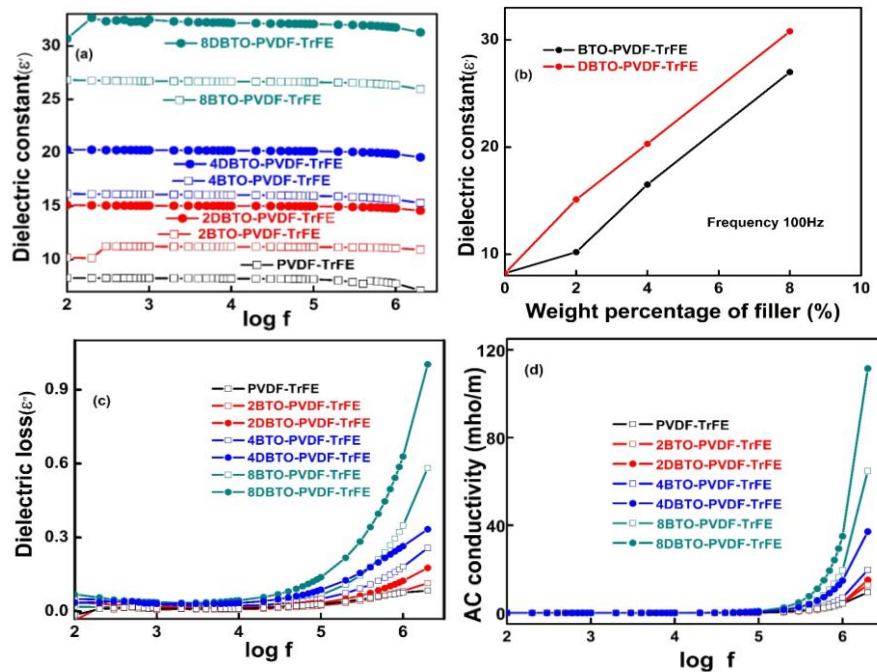


**Figure 13. Frequency dependence of dielectric constant (a), variation of dielectric constant at 100Hz for different BTO/DBTO concentration (b), frequency dependence of dielectric loss (c), frequency dependence of ac conductivity (d) for BTO-PVDF-TrFE and DBTO-PVDF-TrFE films.**

The variation of the dielectric, piezoelectric, ferroelectric, magnetoelectric properties by adding the non-functionalized and functionalized BaTiO<sub>3</sub> filler in the polymer matrix film have been studied. The dielectric parameters were measured in the frequency range of 100 Hz -2 MHz. Fig. 13(a) shows the enhancement of dielectric constant of the films with the increase of BaTiO<sub>3</sub> concentration. The dielectric constant values were found to be well stable over wide frequency range without much decrease at higher frequencies and without much increase at lower frequencies, which generally occurred in nanocomposite samples due to interfacial space charge polarization.<sup>57-60</sup> Fig. 13(b) depicts the variation of dielectric constant for BTO/DBTO-PVDF-TrFE composite film, for different filler concentration at a fixed frequency(100Hz). From the above figure it was clearly evident that, with increase in filler concentration dielectric constant value increases steadily.

Dielectric constant of the neat polymeric sample is found to be 8.4. After addition of the 8% BTO filler, the dielectric constant value increases up to 27 in unfunctionalized BTO composite film and 30.9 for functionalized composite films, respectively. At the same time dielectric loss of the composite films Fig. 13(c) decreases with the increase of filler concentration. The functionalized BaTiO<sub>3</sub> samples showed minimum loss, because dopamine forms a bridge between the nanoparticles and polymer matrix. This results in the reduction of the concentration and movement of the hydroxyl groups on the surface of the nanoparticles. Interestingly, dielectric loss in the composite samples is extremely low, typically below 10% over a wide frequency range for the functionalized samples. On the other hand, ac conductivity Fig. 13(d) is found to be independent of the addition of both BTO and DBTO in the polymer in the low frequency (non-dispersive) regime. The ac conductivity in the dispersive regime (higher frequencies) showed higher value with the increase of filler content in the composite film samples, and functionalization of the BTO has played a significant role on the higher conductivity values with the addition of the filler. Obtained dielectric results were well comparable with the results obtained from the literature by Mendes et.al and R.P.Ummer et.al.<sup>33,50</sup> The material with higher dielectric constant and higher ac conductivity with low loss can be applicable in energy storage systems<sup>35</sup>

### **3.4. Piezoelectric and Ferroelectric properties**

Flexible films with good piezoelectric properties can be used as sensors. We have studied the piezoelectric response of the composite samples, considering the piezoelectric properties in tetragonal structured BaTiO<sub>3</sub> and PVDF-TrFE have been studied in detail in order to explore these materials for sensor applications. The nanocomposites of piezoelectric–polymer having

better piezoelectric performance than the polymers and ceramics has been preferred for the fabrication of piezoelectric nanoenergy generators, sensors, actuators etc.<sup>61,62</sup>

**Table 2. Calculated Piezoelectric coefficient of BTO-PVDF-TrFE and DBTO-PVDF-TrFE films with different filler concentrations in the polymer matrix.**

Sample Name	$d_{33}$ coefficient
PVDF-TrFE	-18pC/N
2BTO-PVDF-TrFE	-20pC/N
4BTO-PVDF-TrFE	-23pC/N
8BTO-PVDF-TrFE	-26pC/N
2DBTO-PVDF-TrFE	-22pC/N
4DBTO-PVDF-TrFE	-25pC/N
8DBTO-PVDF-TrFE	-28pC/N

Piezoelectric coefficient ( $d_{33}$ ) of prepared films are given in the Table 2. Dopamine modified samples shows slightly higher  $d_{33}$  coefficient compared to the non-functionalized samples. The obtained piezoelectric coefficients of the composite films were well comparable with the values obtained from previous literatures by V.S. Nguyen et.al and P. Martins et.al.<sup>61,63</sup>

After studying the piezoelectric properties, the ferroelectric properties of the films have also been studied. The electric field (E) dependence of electric polarization (P) for BTO, PVDF-TrFE, BTO-PVDF-TrFE, and DBTO-PVDF-TrFE samples have been measured by varying frequency (frequency = 1/time period) at constant voltage (Fig. 14). All the samples have showed a good signature of ferroelectric polarization at room temperature.<sup>5,64,65</sup>

The frequency dependence of the P-E loop parameters (electric coercivity ( $E_C$ ) and remanent polarization( $P_R$ ) are shown in Fig. 15. The values of ferroelectric loop parameters observed in our samples are well comparable to the previous literatures.<sup>5,47,66</sup> The following information is of importance for material design and applications of the present materials. In case of space charge controlled polarization in a sample, both polarization and coercive field can increase by decreasing the measurement loop frequency. All the samples have shown an increase in both remanent polarization and coercive field with the decrease of loop frequency. Here the switchable component of electric polarization enhances at lower frequencies. Fig. 15 suggests that remnant polarization of the BTO sample is higher than that in polymer PVDF-TrFE sample, and BTO sample needs higher coercive field to achieve this remnant polarization

than that in polymer PVDF-TrFE sample. On the other hand, remnant polarization and coercive field can be tuned in a wide range for the composite samples. Interestingly, the

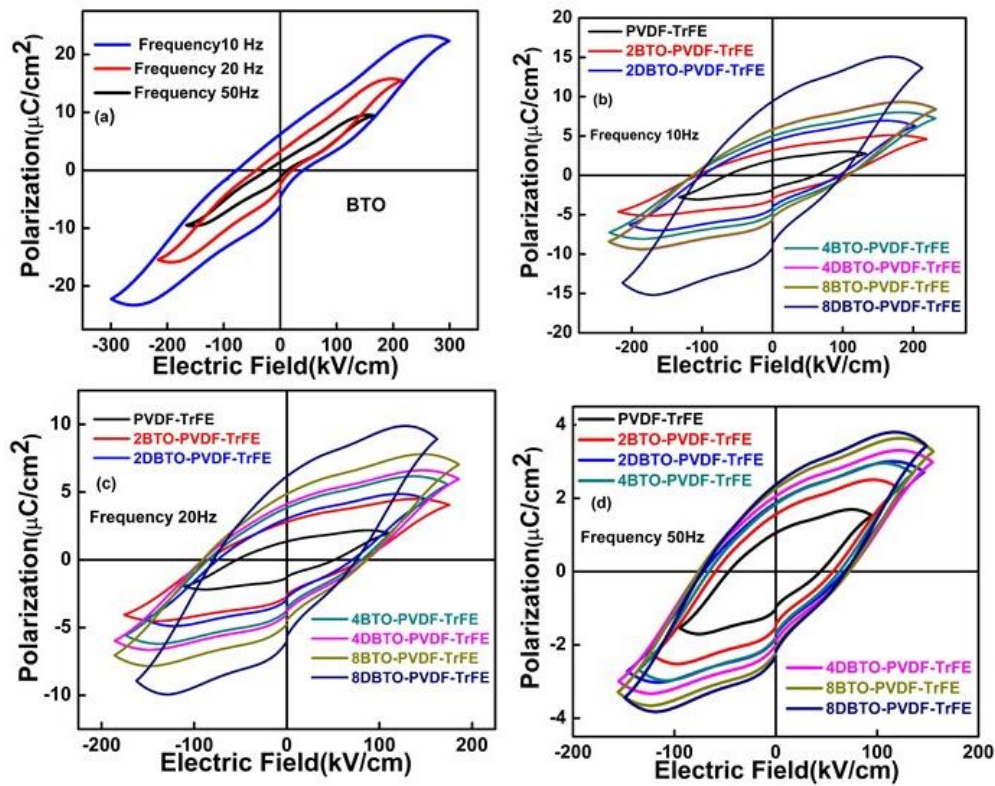


Figure 14. P-E loop of BTO-PVDF-TrFE and DBTO-PVDF-TrFE films at constant field and different frequency (Time period). (a) P-E loop of BTO at different frequencies, (b) P-E loop of composite films at 10 Hz, (c) P-E loop of composite films at 20Hz, (d) P-E loop of composite films at 50Hz.

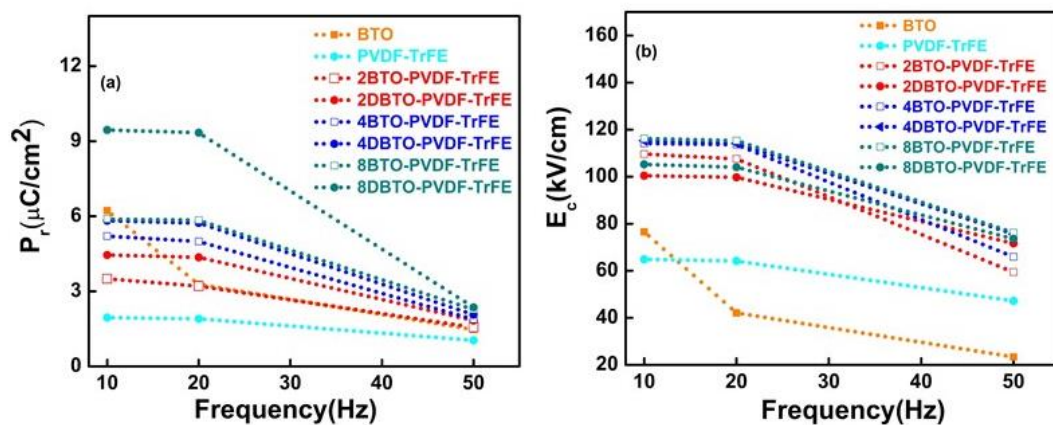


Figure 15. Frequency dependence of the ferroelectric loop parameters, (a) variation of  $P_r$  with loop frequency for BTO/ DBTO -PVDF-TrFE films and (b) Variation of  $E_c$  with loop frequency for BTO/ DBTO -PVDF-TrFE films.

**Table 3: - Calculated ferroelectric loop parameters of BTO-PVDF-TrFE and DBTO-PVDF-TrFE films.**

Sample Name	Ferroelectric Parameters		
	Frequency (Hz)	Pr ( $\mu\text{C}/\text{cm}^{-2}$ )	Ec (MV/m)
PVDF-TrFE	<b>10</b>	1.95	64.25
2BTO-PVDF-TrFE		3.5	109.66
2DBTO-PVDF-TrFE		4.45	100.43
4BTO-PVDF-TrFE		5.21	113.61
4DBTO-PVDF-TrFE		5.71	114.14
8BTO-PVDF-TrFE		5.82	115.21
8DBTO-PVDF-TrFE		9.45	105.23
PVDF-TrFE	<b>20</b>	1.90	64.84
2BTO-PVDF-TrFE		3.21	107.56
2DBTO-PVDF-TrFE		4.36	99.79
4BTO-PVDF-TrFE		4.99	113.63
4DBTO-PVDF-TrFE		5.73	114.14
8BTO-PVDF-TrFE		5.85	115.17
8DBTO-PVDF-TrFE		9.36	116.04
PVDF-TrFE	<b>50</b>	1.04	47.21
2BTO-PVDF-TrFE		1.56	59.42
2DBTO-PVDF-TrFE		1.83	71.64
4BTO-PVDF-TrFE		1.88	65.95
4DBTO-PVDF-TrFE		2.06	75.63
8BTO-PVDF-TrFE		2.27	76.21
8DBTO-PVDF-TrFE		2.36	73.60

tuning property of ferroelectric parameters is higher with enhanced values in the functionalized composite samples than that in non-functionalized samples. Also it should be noted that maximum value of polarization ( $P_{\max}$ ) at 10 Hz  $2.78\mu\text{C}/\text{cm}^2$ ,  $8.39\mu\text{C}/\text{cm}^2$  and  $13.63\mu\text{C}/\text{cm}^2$  for neat PVDF-TrFE, 8BTO-PVDF-TrFE, 8DBTO-PVDF-TrFE, respectively. It can be found that the functionalization of BTO particles play a crucial role in improving the ferroelectric performance of the composite films. Ferroelectric loop parameters of the composite films corresponding to different frequencies are shown in table 3.

### 3.5. Magnetoelectric properties

After confirmation of the stable dielectric parameters, piezoelectric coefficient, and good signature of ferroelectric properties, the ME coupling in the composite samples has been studied. Magnetoelectric coupling coefficient for a.c and d.c field were measured for different BTO/DBTO concentration in PVDF-TrFE matrix. When BTO/DBTO-PVDF-TrFE nanocomposites films were placed in a magnetic field, the field induces a dimensional change in the magnetostrictive BTO (induced magnetism) <sup>28</sup> which is transferred to the nearby piezoelectric polymer matrix.

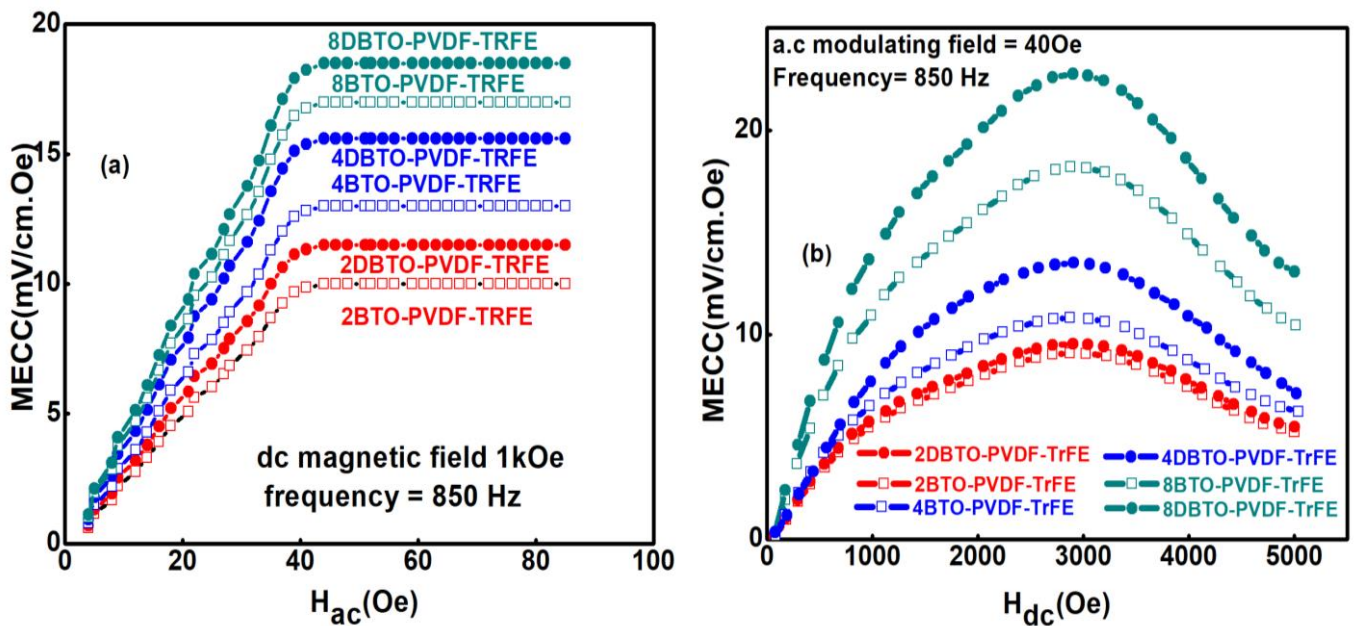


*Figure 16. The variation of magnetoelectric (ME) coupling coefficient measured across the samples under the application of (a) AC and (b) DC magnetic fields for BTO-PVDF-TrFE, DBTO-PVDF-TrFE films.*

As a result, a mechanically induced alteration in electric polarization occurs and hence magnetoelectric voltage is produced. For the direct ME effect in composites, the ME

coupling coefficient is defined by  $\alpha = MECC = dE/dH = (1/t) (dV/dH) = V_{out}/ht$ , where  $V_{out}$  represents the ME voltage produced across the sample surface,  $h$  denotes the amplitude of the applied a.c magnetic field, and  $t$  is the thickness of the sample.<sup>67-71</sup>

For the a.c measurement, magnetoelectric coupling coefficient (MECC) increases to the magnetic field 40 Oe (optimum magnetic field) after that  $\alpha$  value remains constant. The maximum value of  $MECC_{ac}$  ( $\alpha_{ac}$ ) is found to be 18.2mV/cm. Oe for the 8DBTO-PVDF-TrFE film. From the d.c measurement, it is found that  $MECC_{dc}$  ( $\alpha_{dc}$ ) value increases with increase in dc magnetic field to 2800Oe (optimum magnetic field) and after that  $MECC(\alpha)$  value decreases slightly. The maximum value of  $MECC_{dc}$  ( $\alpha_{dc}$ ) is obtained for 8DBTO-PVDF-TrFE film and is found to be 22.2mV/cm.Oe. In both a.c and d.c measurements, as BTO/DBTO content in PVDF-TrFE increases, the magnetoelectric coupling coefficient also increases. It may be mentioned that ME coupling was absent in the pure polymeric PVDF-TrFE sample because the polymer is ferroelectric but the magnetic component is completely absent.

The magnetoelectric response in BTO/ DBTO-PVDF-TrFE composites films were quite analogous to the behaviour observed for P(VDF-TrFE)/CoFe<sub>2</sub>O<sub>4</sub>. Among the present composite system 8DBTO-PVDF-TrFE shows maximum magnetoelectric coupling even at a magnetic field intensity of 2800 Oe which is suited for technological applications. Moreover, the above composite system exhibits better magnetoelectric response when compared to the existing systems Fe<sub>3</sub>O<sub>4</sub>/P(VDF-TrFE), NiFe<sub>2</sub>O<sub>4</sub>-PVDF, CoFe<sub>2</sub>O<sub>4</sub>-PVDF,  $\delta$ -FeO(OH)/P(VDF-TrFE), and Ni<sub>0.5</sub>Zn<sub>0.5</sub>Fe<sub>2</sub>O<sub>4</sub>/P(VDF-TrFE), composite systems.<sup>34-38,67-71</sup>

#### 4. Conclusions

Barium titanate nanoparticles were synthesized by Pechini method and functionalized using dopamine hydrochloride. Particle size in the nanometer regime was confirmed using FE-SEM and TEM analysis. The provided FE-SEM images itself are solid evidences for the changes in shape of the synthesized BaTiO<sub>3</sub> nanoparticles from cubic/tetragonal to spherical form after functionalization. The FTIR and HR-TEM results also confirms the successful functionalization of dopamine over the BTO surface. Two sets of BaTiO<sub>3</sub>/PVDF-TrFE nanocomposites were prepared by the addition of both functionalized as well as non-functionalized BaTiO<sub>3</sub> into the PVDF-TrFE polymer matrix by varying the filler concentration. Polar  $\beta$ -phase of the polymer remains unaltered by the addition of tetragonal BaTiO<sub>3</sub> nanoparticles. Dopamine coating on the surface of the BaTiO<sub>3</sub> passivates the filler surface and promotes the homogeneous dispersion of the nanoparticles in the polymer matrix.

The dielectric, piezoelectric, ferroelectric, and magnetoelectric properties have been studied and found that the properties are enhanced by increasing the filler content in the polymer matrix. Considerable enhancement in the electrical properties were observed in functionalized samples and can be attributed to the better compatibility between the interfaces of filler BaTiO<sub>3</sub> nanoparticles and polymer matrix. It could also be noticed that the composites containing functionalized nanoparticles were having far lower aggregation compared to its counterpart. The thermal conductivity was found to increase with filler concentration whereas the specific heat capacity was decreasing in the composite samples. The DBTO-PVDF-TrFE composites showed better thermal conductivity compared to BTO-PVDF-TrFE films. The ac and dc magnetoelectric coupling of the composite films were found to be enhanced with an increase in BTO/DBTO concentration. It can be concluded that the present nanocomposite with functionalized BaTiO<sub>3</sub> nanoparticles as the additive could be a promising candidate for the development of smart energy storage, magnetoelectric as well as energy harvesting device applications.

### **Acknowledgement**

The authors A.M, N.K, K.M.S, and S.T are thankful to Centre for Materials for Electronics Technology (C-MET), Thrissur for piezoelectric measurements, Cochin University of Science and Technology, University of Kerala, India. The financial support from UGC-Government of India through SAP, BRS Schemes and DST-Government of India through FIST program to SPAP is also gratefully acknowledged. One of the authors JMS is thankful to UGC for the fellowship under the scheme DSK-PDF. The authors would like to acknowledge the financial support from DST- Govt. of India through Nano Mission and PURSE schemes.

### **References**

- 1) Zhang, J., Sun, W., Zhao, J., Sun, L., Li, L., Yan, X.J., Wang, K., Gu, Z.B., Luo, Z.L., Chen, Y. and Yuan, G.L., 2017, *ACS Applied Materials & Interfaces*, 9(30),25397-25403.
- 2) X. Huang, P. Jiang, *Advanced Materials*, 2015,27(3),546-54.
- 3) H. Luo, D. Zhang, C. Jiang, X. Yuan, C. Chen, Z. Kechao, *ACS applied materials & interfaces*, 2015,7(15),8061-9.
- 4) G. Wang, X. Huang, P. Jiang, *ACS applied materials & interfaces*, 2015,7(32),18017-27.
- 5) J. Fu, Y. Hou, M. Zheng, Q. Wei, M. Zhu, H. Yan, *ACS applied materials & interfaces*. 2015 ,7(44),24480-91.

- 6) G. Wang, X. Huang, P. Jiang, *ACS Applied Materials & Interfaces*, 2017, 9(8), 7547-55.
- 7) L. Xie, X. Huang, Y. Huang, K. Yang, P. Jiang, *The Journal of Physical Chemistry C*, 2013, 117(44), 22525-37.
- 8) M. Zhu, X. Huang, K. Yang, X. Zhai, J. Zhang, J. He, P. Jiang, *ACS applied materials & interfaces*, 2014, 6(22), 19644-54.
- 9) Z.M Dang, J.K Yuan, S.H Yao, R.J Liao, *Advanced Materials*, 2013, 25(44), 6334-65.
- 10) J. Li, S. I Seok, B. Chu, F. Dogan, Q. Zhang, Q. Wang, *Advanced Materials*, 2009, 21(2), 217-21.
- 11) K. Yang, X. Huang, Y. Huang, L. Xie, P. Jiang, *Chemistry of Materials*, 2013, 25(11), 2327-38.
- 12) D. Wang, Y. Bao, J. W Zha, J. Zhao, Z.M Dang, G.H. Hu, *ACS applied materials & interfaces*, 2012, 4(11), 6273-9.
- 13) Mandal, D., Henkel, K. and Schmeisser, D., *Physical Chemistry Chemical Physics*, 2014, 16(22), pp.10403-10407.
- 14) Jin, J., Zhao, F., Han, K., Haque, M.A., Dong, L. and Wang, Q., *Advanced Functional Materials*, 2014, 24(8), pp.1067-1073.
- 15) Mao, Y., Zhao, P., McConohy, G., Yang, H., Tong, Y. and Wang, X. *Advanced Energy Materials*, 2014, 4(7).
- 16) Ghosh, S.K., Biswas, A., Sen, S., Das, C., Henkel, K., Schmeisser, D. and Mandal, D., *Nano Energy*, 2016, 30, pp.621-629.
- 17) M. Zhu, X. Huang, K. Yang, X. Zhai, J. Zhang, J. He, P. Jiang, *ACS applied materials & interfaces*, 2014, 6(22), 19644-54.
- 18) Furukawa, T., *Phase Transitions: A Multinational Journal*, 1989, 18(3-4), pp.143-211.
- 19) Naber, R.C., Tanase, C., Blom, P.W., Gelinck, G.H., Marsman, A.W., Touwslager, F.J., Setayesh, S. and De Leeuw, D.M., *Nature Materials*, 2005, 4(3), pp.243-248.
- 20) Müller, K., Henkel, K., Paloumpa, I. and Schmeißer, D., *Thin Solid Films*, 2007, 515(19), pp.7683-7687.
- 21) M. Baniasadi, Z. Xu, S. Hong, M. Naraghi, M. Minary-Jolandan, *ACS applied materials & interfaces*, 2016, 8(4), 2540-51.
- 22) S. Sharma, *Adv. Mater. Lett*, 2013, 4, 522-33.
- 23) Z. Fu, W. Xia, W. Chen, J. Weng, J. Zhang, Y. Jiang, G. Zhu, *Macromolecules*, 2016, 49(10), 3818-25.

- 24) J.E Garcia, *Materials*, 2015, 8(11),7821-36.
- 25) N.R. Alluri, B. Saravanakumar, S.J Kim, *ACS applied materials & interfaces*,2015,7(18),9831-40.
- 26) Y. Yan, J. E Zhou, D. Maurya, Y. U Wang, S. Priya, *Nature communications*,2016,7.
- 27) X. Wang, C. N Xu, H. Yamada, K. Nishikubo, X.G. Zheng, *Advanced Materials*, 2005 ,17(10),1254-8.
- 28) T. Woldu, B. Raneesh, M.R. Reddy, N. Kalarikkal, *RSC Advances*,2016,6(10),7886-92.
- 29) Y. Li, X. Huang, Z. Hu, P. Jiang, S. Li, T. Tanaka, *ACS applied materials & interfaces*,2011,3(11),4396-403.
- 30) L. Shaohui, Z. Jiwei, W Jinwen, X. Shuangxi, Z. Wenqin, *ACS applied materials & interfaces*, 2014 ,6(3),1533-40.
- 31) Y. Song, Y. Shen, H. Liu, Y. Lin, M. Li, C.W Nan, *Journal of Materials Chemistry*, 2012,22(16),8063-8.
- 32) V.K Thakur, R.K Gupta, *Chemical reviews*, 2016, 116(7),4260-317.
- 33) Mendes.S. F, Costa, C.M., Caparrós, C., Sencadas, V. and Lanceros-Méndez, S., *Journal of Materials Science*, 2012,47(3), 1378-1388.
- 34) Martins, P., Lopes, A.C. and Lanceros-Mendez, S., *Progress in polymer science*, 2014,39(4), pp.683-706.
- 35) Mendes, S.F., Costa, C.M., Sencadas, V., Nunes, J.S., Costa, P., Grégório, R. and Lanceros-Méndez, S., *Applied Physics A*, 2009,96(4), 899-908,
- 36) Martins, P. and Lanceros-Méndez, S., Polymer-based magnetoelectric materials. *Advanced Functional Materials*, 2013,23(27), 3371-3385.
- 37) Martins, P., Lasheras, A., Gutierrez, J., Barandiaran, J.M., Orue, I. and Lanceros-Mendez, S., 2011, *Journal of Physics D: Applied Physics*, 44(49), 495303.
- 38) Martins, P., Kolenko, Y.V., Rivas, J. and Lanceros-Mendez, S., 2015, *ACS applied materials & interfaces*, 7(27), 15017-15022.
- 39) G. Wang, X. Huang, P. Jiang, *ACS Applied Materials & Interfaces*, 2017 ,9(8),7547-55.
- 40) V.KumaráThakur, E. JináTan, P. SeeáLee, *RSC Advances*, 2011,1(4),576-8.
- 41) Y. Xie, Y. Yu, Y. Feng, W. Jiang, Z. Zhang, *ACS Applied Materials & Interfaces*, 2017.

- 42) M.S Jayalakshmy, J. Philip, *Journal of Polymer Research*, 2015,22(3),1-11.
- 43) M.S Jayalakshmy, J. Philip, *Sensors and Actuators A: Physical*,2014, 206,121-6.
- 44) B. Luo, X. Wang, Y. Wang, L.Li, *Journal of Materials Chemistry A*, 2014,2(2),510-9.
- 45) D. Yang, M. Ruan, S. Huang, Y. Wu, S. Li, H. Wang, X Ao, Liang Y, Guo W, Zhang L, *RSC Advances*, 2016,6(93),90172-83.
- 46) D. Yang, M. Tian, D. Li, W. Wang, F. Ge, L. Zhang, *Journal of Materials Chemistry A*. 2013;1(39):12276-84.
- 47) U. Valiyaneerilakkal, A. Singh, C. K Subash, S.M Abbas, S. Varghese,2015, *Polymer Composites*.
- 48) Biswas, A., Henkel, K., Schmeisser, D. and Mandal, D., *Phase Transitions*, 2017, 90(12), pp.1205-1213.
- 49) Mandal, D., Henkel, K. and Schmeisser, D., *The Journal of Physical Chemistry B*, 2011, 115(35), pp.10567-10569.
- 50) R. P Ummer, B. Raneesh, C. Thevenot, D. Rouxel, S. Thomas, N. Kalarikkal, *RSC Advances*,2016,6(33),28069-80.
- 51) J. Liu, G. Cao, Z. Yang, D. Wang, D. Dubois, X. Zhou, G. L Graff, L. R. Pederson, J.G Zhang, *ChemSusChem*,2008,1(8-9),676-97.
- 52) Y. Li, X. Huang, Z. Hu, P. Jiang, S. Li, T. Tanaka, *ACS applied materials & interfaces*, 2011,3(11),4396-403.
- 53) X. Huang, T. Iizuka, P. Jiang, Y. Ohki, T. Tanaka, *The Journal of Physical Chemistry C*, 2012,116(25),13629-39.
- 54) J.M. Sudhakaran, J. Philip, *Journal of Applied Polymer Science*,2015, 132(28).
- 55) S. Siddabattuni, T.P Schuman, F. Dogan, *ACS applied materials & interfaces*, 2013,5(6),1917-27.
- 56) H. Kim, A.A Abdala, C.W Macosko, *Macromolecules*, 2010 ;43(16),6515-30.
- 57) G. Wang, *ACS applied materials & interfaces*. 2010,2(5),1290-3.
- 58) Y. Feng, W. L Li, Y. F Hou, Y. Yu, W. P. Cao, T.D. Zhang, W.D. Fei, *Journal of materials chemistry C*, 2015;3(6),1250-60.
- 59) K. Yu, K. Bai, Y. Zhou, Y. Niu, H. Wang, *Applied Physics Letters*, 2014 ,104(8),082904.
- 60) L. Xie, X. Huang, K. Yang, S. Li P. Jiang, *Journal of Materials Chemistry A*, 2014, 2(15),.5244-5251.

- 61) V.S. Nguyen, D. Rouxel, M. Meier, B. Vincent, A. Dahoon, S. Thomas, F.D Santos, *Polymer Engineering & Science*, 2014,54(6),1280-8.
- 62) X. Ren, H. Fan, Y. Zhao, Z. Liu, *ACS Applied Materials & Interfaces*, 2016,8(39),26190-7.
- 63) Martins, P., Gonçalves, R., Lanceros-Mendez, S., Lasheras, A., Gutiérrez, J. and Barandiarán, J.M., 2014, *Applied Surface Science*, 313, 215-219.
- 64) H. Pan, Y. Zeng, Y. Shen, Y.H. Lin, C.W. Nan, *Journal of Applied Physics*, 2016, 119(12),124106.
- 65) A.G. Lone, and R.N. Bhowmik, *Journal of Magnetism and Magnetic Materials*, 2015,379, pp.244-255.
- 66) Y. Song, Y. Shen, H. Liu, Y. Lin, M. Li, C.W. Nan, *Journal of Materials Chemistry*,2012,22(32),16491-8.
- 67) Chaudhuri, A. and Mandal, K., 2015, *Journal of Magnetism and Magnetic Materials*, 377,441-445.
- 68) Prabhakaran, T. and Hemalatha, J., *RSC Advances*, 2016, 6(90), 86880-86888.
- 69) Durgaprasad, P. and Hemalatha, J., 2017, *Journal of Magnetism and Magnetic Materials*.
- 70) Gutiérrez, J., Lasheras, A., Barandiarán, J.M., Gonçalves, R., Martins, P. and Lanceros-Méndez, S., 2015. *IEEE Transactions on Magnetics*, 51(11), 1-4.
- 71) B. Raneesh, A. Saha, N. Kalarikkal, *Radiation Physics and Chemistry*,2013, 89,28-32.